16th Australasian Fluid Mechanics Conference
Crown Plaza, Gold Coast, Australia
2-7 December 2007

Electrokinetic Flow Resistance in Pressure-driven Liquid Flow through a Slit-like Microfluidic Contraction

Malcolm R. Davidson, Dalton J. E. Harvie and Petar Liovic

Department of Chemical & Biomolecular Engineering
The University of Melbourne, Melbourne, Victoria, 3010 AUSTRALIA

Abstract

The electrokinetic flow resistance (electroviscous effect) in steady state, pressure-driven liquid flow in a slit-like microfluidic contraction at low Reynolds number is predicted using a finite volume numerical method. A uniform charge density is assumed on the channel walls and the liquid is taken to be a symmetric 1:1 electrolyte. Predictions of the apparent viscosity are shown to be well described by a simple theory that calculates the pressure drop along the channel by adding the pressure losses in the inlet, contraction and outlet sections (based on the classical electrokinetic flow solution in a uniform slit) to the entry and exit losses due to the contraction. These entry and exit losses are approximated using the low Reynolds number analytical solution for a slit orifice without electrokinetic effects.

Introduction

Electrokinetic phenomena develop when a charged surface is brought into contact with an ionic liquid. A charged channel wall attracts counter-ions in the liquid and a diffuse electric double layer (EDL) forms in which the concentration of counterions decreases away from the wall. In pressure-driven flow these counter-ions are carried downstream setting up a current that generates a potential field within the channel. This streaming potential, in turn, induces an electrokinetic force that opposes the primary liquid flow, thereby increasing the flow resistance and the apparent viscosity (electroviscous effect) [9, 12]. The effect only becomes significant for channel widths on the scale of microns when the EDL thickness is a non-neglibible fraction of the channel width (EDL thickness can range from nanometres to one or two microns, depending on the ionic concentration and electrical properties of the liquid [12]). In recent years there has been an explosion of research activity related to micro-electro-mechanical systems (MEMS) [6]. Many new and existing devices being developed for applications in biotechnology involve the flow of gas or liquid in microchannels [19].

Modelling studies of the electroviscous effect in channels of uniform cross-section have included slit-like channels [13, 14, 4], and channels whose cross-sections are cylindrical [1, 2], rectangular [15, 11] and elliptic [8]. However non-uniform geometries such as contractions and T-junctions are common microfluidic elements. Very recently, the authors published a numerical study of the electroviscous effect in the 1:4 slit-like contraction-expansion [5] shown in figure 1. The current paper presents some results not previously shown.

Model Description

Consider a symmetric 1:1 electrolyte solution of constant viscosity (μ) and density (ρ), for which the anions and cations (specified by $+$ and $-$, respectively) have equal diffusivities D and valencies z, with the bulk ionic concentration of each species denoted by n_o. We investigate the two dimensional flow of the electrolyte solution through the 1:4 slit-like contraction shown in Fig 1. The half-width of the inlet and outlet channels (taken to be equal) is denoted by W, and the mean inflow velocity is denoted by $\bar{V}$. The channel walls are assumed to carry a net immobile electrostatic charge of surface density σ.

The velocity, length, time, number density of anions and cations, and electrical potential are scaled according to $\bar{V}$, W, $W/\bar{V}$, n_o, kT/ze, respectively, where e is the elementary charge, k is the Boltzmann constant and T denotes temperature. The dimensionless equations governing the flow, the electric field and the ion transport are then:

$$\nabla^2 U = -\frac{1}{2}K^2(n_+ - n_-) \tag{1}$$

$$\frac{\partial n_+}{\partial t} + \nabla\cdot(\mathrm{v}n_+) = \frac{1}{\mathrm{ReSc}}\left[\nabla^2 n_+ + \nabla\cdot(n_+\nabla U)\right] \tag{2}$$

$$\frac{\partial n_-}{\partial t} + \nabla\cdot(\mathrm{v}n_-) = \frac{1}{\mathrm{ReSc}}\left[\nabla^2 n_- - \nabla\cdot(n_-\nabla U)\right] \tag{3}$$

$$\frac{\partial \mathrm{v}}{\partial t} + \nabla\cdot(\mathrm{vv}) = -\nabla P + \frac{1}{\mathrm{Re}}\nabla\cdot\left[\nabla\mathrm{v} + (\nabla\mathrm{v})^T\right] - \frac{\mathrm{B}K^2}{\mathrm{Re}^2}(n_+ - n_-)\nabla U \tag{4}$$

$$\nabla\cdot\mathrm{v} = 0 \tag{5}$$

where the Poisson equation 1 relates the total electrical potential U at a point to the local charge density, the Nernst-Planck equations 2 and 3 describe conservation of each ion species (n_+ and n_- are the dimensionless number of positive and negative ions per unit volume, respectively), and equations 4 and 5 are the usual Navier-Stokes equations, but with an additional body force in the momentum equation that is the electrical force due to free charges.

The dimensionless groups in the above equations are

$$\mathrm{Re} = \frac{\rho\bar{V}W}{\mu}, \quad \mathrm{Sc} = \frac{\mu}{\rho D}, \quad \mathrm{B} = \frac{\rho k^2T^2\varepsilon_0\varepsilon}{2z^2e^2\mu^2}, \quad K^2 = \frac{2z^2e^2n_oW^2}{\varepsilon_0\varepsilon kT} \tag{6}$$

where Re and Sc are the familiar Reynolds number and Schmidt number, K is the dimensionless inverse Debye length (i.e. a measure of the ratio of the channel width W to the EDL thickness), and B is a parameter that is fixed for a given liquid at a specified temperature.

The surface charge density equals a jump in the dielectric displacement normal to the boundary between the liquid and the wall material. Since most liquids in biotechnology are aqueous-based, and water has a dielectric constant of about 80 compared

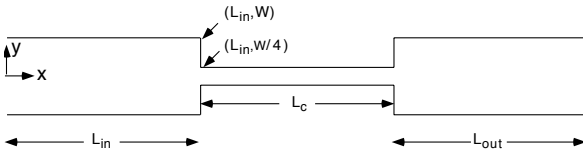

Figure 1: Schematic of the 1:4 contraction-expansion flow geometry.

with approximately 3 for glass or PMMA/PDMS, we ignore the dielectric displacement in the wall material. In that case, the wall boundary condition for the electrical potential is (in dimensionless form)

$$\frac{\partial U}{\partial n} = S \tag{7}$$

where n denotes the outwards normal at the channel wall (we also use n for ion concentration, but it is always subscripted in that case), and the dimensionless surface charge density

$$S = \frac{ze\sigma W}{\varepsilon_0 \varepsilon k T} \tag{8}$$

Other wall boundary conditions are zero flux of ions normal to the wall and the no slip velocity condition. The velocity and ion concentrations at the inlet are taken to be those for steady, fully developed electroviscous flow in a uniform two-dimensional slit [3, 5]. In that case, the net axial current is zero. At steady state, the total current passing through the outlet cross-section also becomes zero. The axial potential gradient at the channel outlet is taken to be uniform and is chosen to satisfy Gauss's law over the flow domain. The axial pressure gradient at the outlet is chosen to ensure global mass conservation, and axial gradients in the ion concentrations and axial velocity are taken to be zero there.

Numerical Considerations

We extend a single phase version of the transient, explicit, two-fluid finite volume method described by Rudman [16] to include electrokinetic flow, and use this to integrate to a steady state. The authors have previously used the Rudman algorithm for various transient, two fluid flows with interfaces, but without electrokinetics [7]. Using the Rudman code here will make it more convenient to extend the work to electrokinetic flows with deforming interfaces in the future.

A uniform staggered grid with 32 mesh cells over the half-width W of the inlet is used. A semi-implicit time stepping procedure that allows for larger timesteps at low Reynolds numbers is used to speed up the computation of the steady state. Time step constraints required for numerical stability include limits involving the electrokinetic parameters as well as the Courant condition. Details can be found in Davidson and Harvie [5].

Results and Discussion

We present selected results for $\mathrm{B} = 2.34 \times 10^{-4}$, $\mathrm{Sc} = 1000$ and $\mathrm{Re} = 0.01$. The first two parameter values are derived using the properties of water and a temperature of 298 K. The geometry is chosen with $L_{in}/W = L_{out}/W = L_c/W = 5$ (see figure 1). Figure 2 shows the charge distribution for $S = 16$. Results for negative values of S can be obtained by setting new values of U, n_+ and n_- equal to $-U$, n_- and n_+, respectively. The figure shows that the region of negative charge that is induced by the positive surface charge expands away from the wall, and the net charge within the contraction becomes more negative, as K decreases and the EDL becomes thicker. The charge is more negative in the contraction than it is in the inlet and outlet sections. The variation in the net charge with K and a comparison of the charge within the contraction with that in the inlet and outlet sections is quantified more clearly in figure 3 which shows the charge on the centreline.

Figure 4 shows the electrical potential along the centreline. The potential decreases in the direction of flow because of the advection of negative charge along the channel. As K decreases, the magnitude of the potential gradient becomes greater, since the EDLs occupy a greater fraction of the channel width so that

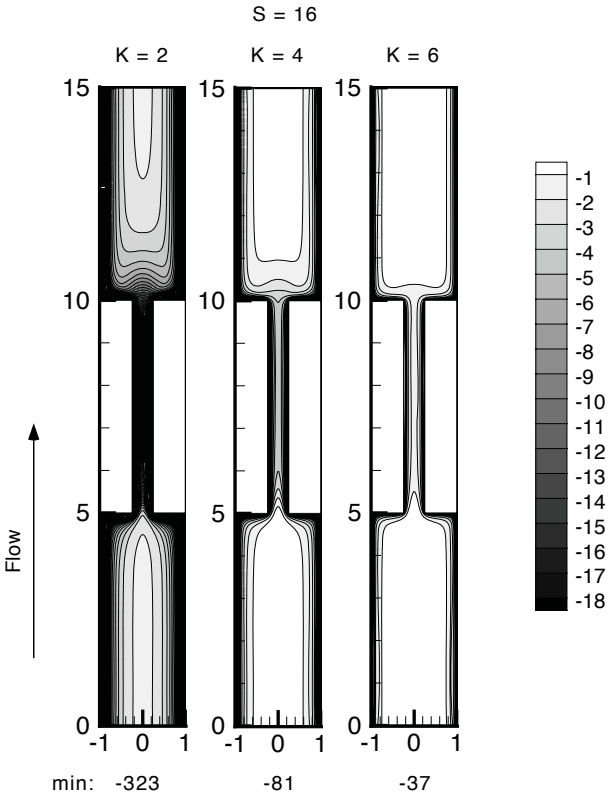

Figure 2: Dimensionless charge distribution $(n_+ - n_-)$ for surface charge density parameter $S = 16$ and different values of scaled inverse Debye length K.

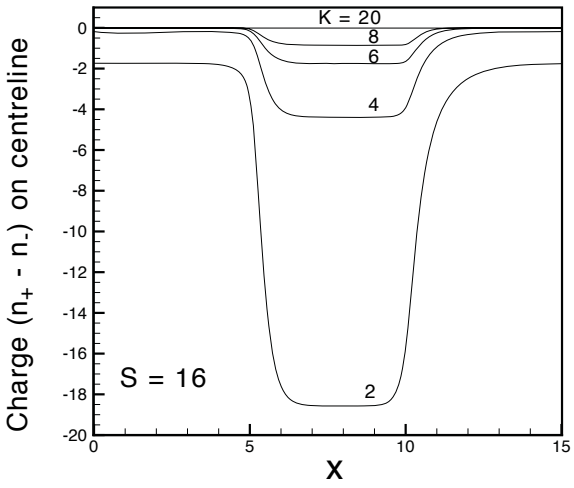

Figure 3: Dimensionless charge $(n_+ - n_-)$ on the centreline for surface charge density parameter $S = 16$ and different values of scaled inverse Debye length K.

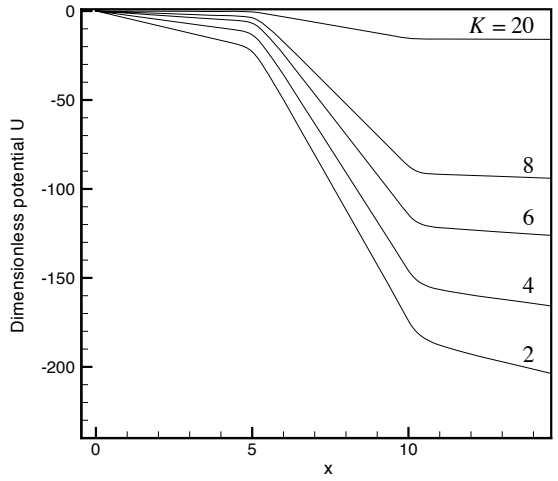

Figure 4: Dimensionless potential U on the centreline for surface charge density parameter $S = 16$ and different values of scaled inverse Debye length K.

more counterions are transported by the flow. The potential gradient is also greatest in the contraction for the same reason.

In figure 5 the lateral profiles of electrical potential are compared with those for a uniform slit having the same width as the local channel width. Comparisons are made at locations half way along the contraction and outlet sections for surface charge parameter $S = 16$. The modified potential $U(x,y) - U(x,0) + \psi(0)$ is compared with $\psi(y)$ where $\psi(y)$ is the EDL potential in a uniform channel (see [5] for details). This has the effect of removing axial variation in U and forcing the value of the modified potential to equal $\psi(0)$ on the axis; the two curves are then compared for $y > 0$. The predicted lateral profiles are effectively coincident with their uniform slit counterparts. The same applies for lateral profiles of ion concentrations and axial velocity (not shown).

Apparent Viscosity

The additional flow resistance due to the electrical force in equation 4 results in a pressure drop ΔP that is larger than the pressure drop ΔP_o that occurs when the electrical force is absent. Here we quantify this using an apparent viscosity μ_{eff} which is the viscosity of a fluid with no electrical forcing that will achieve the pressure drop ΔP for fixed flow rate. For low Reynolds number, as is the case here, $\mu_{eff}/\mu = \Delta P/\Delta P_o$ in steady flow. Figure 6 shows the variation for various K and S values. The trends are the same as for a uniform channel [4] with μ_{eff}/μ decreasing towards 1 with increasing K, and decreasing overall as S becomes smaller.

The continuous lines in figure 6 are an approximation to μ_{eff}/μ based on the overall pressure drop, estimated as

$$\Delta P_m = \Delta P_{io} + \Delta P_c + \Delta P_e \tag{9}$$

where ΔP_{io} is the pressure drop due to fully developed electroviscous flow for a uniform slit in the sections before the contraction and after the expansion of length (length $L_{in} + L_{out}$ and half-width W), ΔP_c is the corresponding pressure drop in a slit having the length of the contraction (L_c) and half-width $W/4$. The excess pressure drop ΔP_e is obtained from the analytical creeping flow solution [18] for a slit orifice in an infinite uncharged planar wall. An expression for electrokinetic orifice flow would be preferable but none is available. The uniform slit

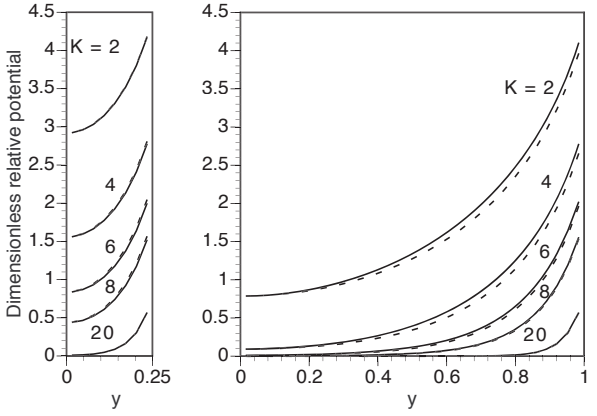

Figure 5: Comparison between numerical predictions for the dimensionless EDL portential for the expansion-contraction (solid lines) and classical results for a uniform slit having a width the same as the contraction or the outlet (dashed lines) when the surface charge parameter $S = 16$. Transverse profiles are shown at locations half way along the contraction and outlet sections.

solution is summarised in [5]. The dimensionless excess pressure drop is given by

$$\Delta P_e = \frac{16}{\pi d^2 \mathrm{Re}} \tag{10}$$

where d denotes the contraction ratio (here $d = 0.25$). The advantage of using this simple model of pressure drop to estimate the apparent viscosity is that it is more convenient than a full numerical simulation of the flow. Sisavath et al. [17] successfully used a similar approach to approximate the pressure drop along a tube containing an axisymmetric sudden contraction or expansion, without electrokinetic effects.

Figure 6 compares the apparent viscosity determined from the numerical model (symbols) with that (solid lines) based on the simple model described above. The simple model overestimates the apparent viscosity (flow resistance). This overestimate tends to be larger when the surface charge parameter is greatest ($S = 16$) and lower when it is smallest ($S = 4$). Also the simple model becomes a very good approximation as K increases.

The difference between the predictions of the simple model and the simulation are explained by the absence of electrokinetic effects in the expression for the excess pressure drop. This absence means that the simple model does not account for flow resistance due to surface charge over the forward and rear facing sections of the wall at the entrance and exit of the contraction. Along the step located at $x = L_{in}$, the flow is directed towards the centre line which promotes a positive local potential gradient $\partial U/\partial y$ (for $S > 0$). This is reinforced by the positive potential gradient normal to the outer wall at $y = W$ near $x = L_{in}$ and produces a lateral electrical force that reduces the inwardly directed velocity parallel to the forward facing step. This consequently reduces the wall friction on the step compared to that which occurs when surface charge on the step is ignored. The lateral potential gradient $\partial U/\partial y$ is found to be small along the step located at $x = L_{out}$. This occurs because the flow there now promotes a negative local potential gradient that is opposite to the gradient normal to the outer wall, and these two factors effectively cancel each other. Consequently, there is little influence on wall friction over the step at the contraction exit.

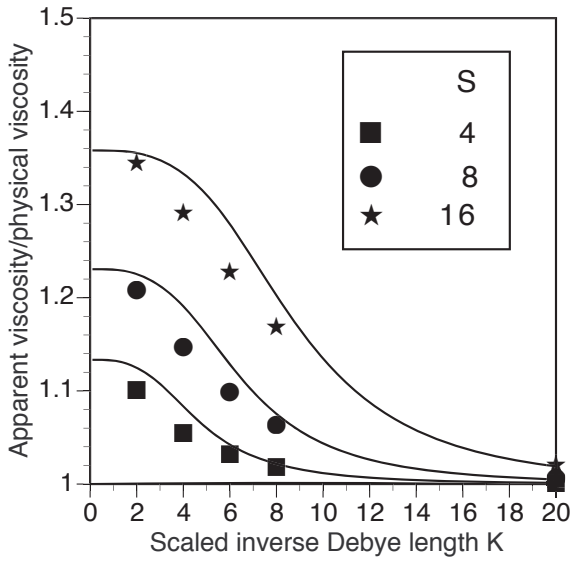

Figure 6: Comparison between numerical predictions (symbols) of the ratio of apparent viscosity to physical viscosity for contraction-expansion flow and corresponding predictions of a simple low Reynolds number model (lines).

Conclusions

The apparent viscosity incorporating flow resistance due to electroviscous effects is predicted for steady state, pressure-driven liquid flow at low Reynolds number in a 1:4 slit-like microfluidic contraction. The two-dimensional electrokinetic flow equations are solved numerically using a finite volume method. The apparent viscosity/physical viscosity ratio decreases towards one with decreasing surface charge density and decreasing EDL thickness, and are the same trends as for a uniform channel.

The apparent viscosity is estimated using a simple theory that approximates the entry and exit losses (excess pressure drop) due to the contraction by the low Reynolds number analytical solution for a slit orifice in a infinite wall without electrokinetic effects. The overall pressure drop (and hence the apparent viscosity) is then approximated by adding the pressure losses in each uniform section of the channel, using the classical fully developed electrokinetic flow solution in a uniform slit, to the estimated excess pressure drop.

The simple theory overestimates the apparent viscosity by up to 5-10 percent, compared with the numerical solution. The reason is that the orifice contribution to the simple model does not include the effect of surface charge on the forward and rear facing steps at the entrance and exit of the contraction. The electrokinetic effect at these steps is to assist, rather than oppose, the flow.

Acknowledgements

This research was supported by the Australian Research Council Grants Scheme.

References

[1] Bowen, W.R. and Jenner, F., Electroviscous Effects in Charged Capillaries, *J. Coll. Interface Sci.*, **173**, 1995, 388–395.

[2] Brutin, D. and Tadrist, L., Modeling of Surface-fluid Electrokinetic Coupling on the Laminar Flow Friction Factor in Microtubes, *Microscale Thermophysical Engineering*, **9**, 2005, 33–48.

[3] Burgreen, D. and Nakache, F.R., Electrokinetic Flow in Ultrafine Capillary Slits, *J. Phys. Chem.*, **68**(5), 1964, 1084–1091.

[4] Chun, M. and Kwak, H.W., Electrokinetic Flow and Electroviscous Effect in a Charged Slit-like Microfluidic Channel with nonlinear Poisson-Boltzmann Field, *Korea-Australia Rheology J.*, **15**(2), 2003, 83–90.

[5] Davidson, M.R. and Harvie, D.J.E., Electroviscous Effects in low Reynolds Number Liquid Flow through a Slit-like Microfluidic Contraction, *Chemical Engineering Science*, **62**, 2007, 4229–4240.

[6] Gad-El-Hak, M. editor *The MEMS Handbook*, second edition, CRC Press, Boca Raton, 2006.

[7] Harvie, D.J.E., Davidson, M.R., Cooper-White, J.J., Rudman, M., A Parametric Study of Droplet Deformation through a Microfluidic Contraction: Shear Thinning Liquids, *Int. J. Multiphase Flow*, **33**, 2007, 545–556.

[8] Hsu, J., Kao, C., Tseng, S., Chen, C., Electrokinetic Flow through an Elliptical Microchannel: Effects of Aspect Ratio and Electrical Boundary Conditions, *J. Coll. Interface Sci.*, **248**, 2002, 176–184.

[9] Hunter, R.J, *Zeta potential in colloid science: Principles and Application*, Academic Press, NY, 1981.

[10] Hunter, R.J, *Foundations of Colloid Science*, Vol. II, Clarendon Press, Oxford, 1989, p. 793.

[11] Li, D., Electro-viscous Effects on Pressure-driven Liquid Flow in Microchannels, *Colloids and Surfaces A*, **195**, 2001, 35–57.

[12] Li, D., *Electrokinetics in Microfluidics*, Interface Science and Technology, Vol. 2 (ed. A. Hubbard), Academic Press, 2004.

[13] Mala, G.M., LI, D. and Dale, J.D., Heat Transfer and Fluid Flow in Microchannels, *Int. J. Heat Mass Transfer*, **40**, 1997a, 3079–3088.

[14] Mala, G.M., LI, D., Werner, C and Jacobasch, H., Flow Characteristics of Water through a Microchannel between two Parallel Plates with Electrokinetic Effects, *Int. J. Heat and Fluid Flow*, **18**(5), 1997b, 489–496.

[15] Ren, L., Li, D. and Qu, W., Electro-viscous Effects on Liquid Flow in Microchannels, *J. Coll. Interface Sci.*, **233**, 2001, 12–22.

[16] Rudman, M., A Volume-tracking Method for Incompressible Multifluid Flows with Large Density Variations, *Int. J. Numer. Methods in Fluids*, **28**, 1998, 357–378.

[17] Sisavath, S., Jing, X., Pain, C.C., Zimmerman, R.W., Creeping flow through an axisymmetric sudden contraction or expansion, *J. Fluids Eng.*, **124**, 2002, 273-278.

[18] Wuest, V.W., Strömung Durch Schlitz- und Lochblenden bei kleinen Reynolds-Zahlen, *Ingen. Archiv.*, **24**, 1954, 357-367.

[19] Whitesides, G. and Stroock, A., Flexible Methods for Microfluidics, *Physics of Fluids*, **54**(6), 2001, 42–48.

Notation

B	$\rho k^2 T^2 \varepsilon_0 \varepsilon / 2 z^2 e^2 \mu^2$
D	diffusivity of positive and negative ions, assumed equal ($m^2 s^{-1}$)
d	contraction ratio
e	elementary charge (C)
k	Boltzmann constant (JK^{-1})
K	dimensionless inverse Debye length $\left[2z^2 e^2 n_o W^2 / \varepsilon_0 \varepsilon k T\right]^{1/2}$
L_{in}	length of inlet section of the channel (m)
L_{out}	length of outlet section of the channel (m)
L_c	length of the contracted section of the channel (m)
n_o	bulk ionic concentration (m^{-3})
n_+, n_-	dimensionless concentrations of positive and negative ions, respectively
n	(no subscript) dimensionless outward normal to the channel wall
P	pressure
Re	Reynolds number $\rho \bar{V} W / \mu$
S	dimensionless surface charge density $ze\sigma W / \varepsilon_0 \varepsilon k T$
Sc	Schmidt number $\mu / \rho D$
T	temperature (K)
t	dimensionless time
U	total dimensionless electrical potential
v	dimensionless liquid velocity
$\bar{V}$	mean inlet velocity (ms^{-1})
W	half-width of the inlet or outlet section of the channel (m)
x, y	axial and transverse coordinates, respectively
z	valence of positive and negative ions, assumed equal

Greek symbols

ε	dielectric constant of the liquid
ε_0	permittivity of free space ($CV^{-1}m^{-1}$)
ΔP	pressure drop
ΔP_o	pressure drop without electrokinetic effects
ΔP_e	pressure drop due to contraction/expansion
ΔP_m	pressure drop predicted by the simple model
ΔP_{io}	pressure drop for fully developed flow in the uncontracted section
ΔP_c	pressure drop for fully developed flow in the contracted section
μ	liquid viscosity (Pa s)
ψ	dimensionless electrostatic potential in a uniform slit
ρ	liquid density ($kg\ m^{-3}$)
σ	surface charge density (Cm^{-2})

Scaling factors

electrical potential	kT/ze
ion concentration	n_o
length	W
pressure	$\rho \bar{V}^2$
time	$W/\bar{V}$
velocity	$\bar{V}$